10

Calendering and lubrication

10.1 An elastic strip between rollers

Many processes involve the passage of a strip or sheet of material through the nip between rollers. In this section we consider the strip to be perfectly elastic and investigate the stresses in the strip, the length of the arc of contact with the roller, the maximum indentation of the strip and the precise speed at which it feeds through the nip in relation to the surface speed of the rollers. If the strip is wide and the rollers are long in the axial direction it is reasonable to assume plane deformation.

The static indentation of a strip by rigid frictionless cylinders was considered briefly in §5.8. The stresses in an elastic strip due to symmetrical bands of pressure acting on opposite faces have been expressed by Sneddon (1951) in terms of Fourier integral transforms. The form of these integrals is particularly awkward (e.g. eq. (5.65)) and most problems require elaborate numerical computations for their solution. However, when the thickness of the strip $2b$ is much less than the arc of contact $2a$ an elementary treatment is sometimes possible. The situation is complicated further by friction between the strip and the rollers. We can analyse the problem assuming (*a*) no friction ($\mu = 0$) and (*b*) complete adhesion ($\mu \to \infty$), but our experience of rolling contact conditions leads us to expect that the arc of contact will, in fact, comprise zones of both 'stick' and 'slip'.

We will look first at a strip whose elastic modulus is of a similar magnitude to that of the rollers, and write

$$C \equiv \frac{(1-\nu_1^2)/E_1}{(1-\nu_2^2)/E_2} = \frac{1+\alpha}{1-\alpha} \tag{10.1}$$

where α is defined by equation (5.3*a*) and 1, 2 refers to the strip and the rollers respectively. If the strip is thick ($b \gg a$) it will deform like an elastic half-space

https://doi.org/10.1017/CBO9781139171731.011 Published online by Cambridge University Press

and the contact stresses will approach those discussed in §8.2. With equal elastic constants the deformation will be Hertzian, for unequal elasticity friction will introduce tangential tractions which, in the absence of slip, will be given by equation (8.15).

At the other extreme, when $b \ll a$, the deformation is shown in Fig. 10.1. The compression of the roller is now much greater than that of the strip so that the pressure distribution again approximates to that of Hertz, viz.

$$p(x) = \frac{2P}{\pi a}(1 - x^2/a^2)^{1/2} \tag{10.2}$$

The strip is assumed to deform with plane sections remaining plane so that the compression at the centre of the strip is given by

$$d = \frac{b(1-\nu_1^2)p(0)}{E_1} = \frac{2b(1-\nu_1^2)P}{\pi a E_1}$$

If the deformed surfaces of the strip are now approximated by circular arcs of radius R', then

$$\frac{1}{R'} = \frac{2d}{a^2} = \frac{4b(1-\nu_1^2)P}{\pi a^3 E_1} \tag{10.3}$$

The rollers are flattened from a radius R to R', so that by equation (4.43)

$$a^2 = \frac{4P(1-\nu_2^2)}{\pi E_2} \Big/ \left(\frac{1}{R} - \frac{1}{R'}\right) \tag{10.4}$$

Eliminating R' from (10.3) and (10.4) gives

$$\left(\frac{a}{a_0}\right)^2 = 1 + C\frac{b}{a} \tag{10.5}$$

Fig. 10.1. A thin elastic strip nipped between elastic rollers.

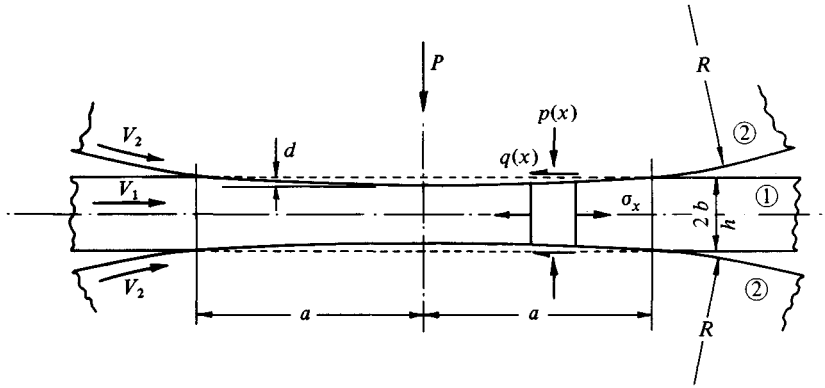

https://doi.org/10.1017/CBO9781139171731.011 Published online by Cambridge University Press

where $a_0 = \{4PR(1-\nu_2^2)/E_2\}^{1/2}$ is the semi-contact-width for a vanishingly thin strip.

With frictionless rollers the longitudinal stress in the strip σ_x is either zero or equal to any external tension in the strip. Due to the reduction in thickness, the strip extends longitudinally, whilst the roller surface compresses according to the Hertz theory, so that in fact frictional tractions $q(x)$ arise (acting inwards on the strip) whether or not the materials of the strip and rollers are the same. For equilibrium of an element of the strip

$$\frac{d\sigma_x}{dx} = \frac{1}{b} q(x) \tag{10.6}$$

Slip between the rollers and the strip is governed by equation (8.3). If there is no slip equation (8.3) reduces to

$$\frac{\partial \bar{u}_{x1}}{\partial x} - \frac{\partial \bar{u}_{x2}}{\partial x} = -\xi \tag{10.7}$$

where ξ is the creep ratio $(V_1 - V_2)/V_2$ of the strip relative to the periphery of the rollers. The longitudinal strain in the strip is given by

$$\frac{\partial \bar{u}_{x1}}{\partial x} = \frac{1-\nu_1^2}{E_1} \left\{ \sigma_x + \frac{\nu_1}{1-\nu_1} p(x) \right\} \tag{10.8}$$

and the surface strain in a roller within the contact arc is given by equation (2.25*a*). For a thin strip we can take the pressure distribution $p(x)$ to be Hertzian given by (10.2). The expressions (10.8) and (2.25*a*) for the strains in the strip and rollers respectively can then be substituted into equation (10.7) which, together with (10.6), provides an integral equation for the tangential traction $q(x)$. This integral equation is satisfied by the traction:

$$q(x) = \left(1 - \frac{4\beta}{1+\alpha}\right) \frac{b}{2a} p_0 \frac{x}{(a^2 - x^2)^{1/2}} \tag{10.9}$$

where β is defined in equation (5.3*b*). This expression for $q(x)$ is satisfactory away from the edges of the contact, but the infinite values at $x = \pm a$ are a consequence of assuming plane sections remain plane. The traction falls to zero, in fact, at the edges.

A complete numerical analysis of this problem has been made by Bentall & Johnson (1968) for a range of values of b/a; the results are shown in Fig. 10.2. The contact pressure is close to a Hertzian distribution for all values of b/a. The frictional traction is zero at the extremes of both thick and thin strips; it reaches a maximum when $b/a \approx 0.25$. Although $q(x)$ falls to zero at $x = \pm a$, in the absence of slip the ratio $q(x)/p(x)$ reaches high values. This implies that some micro-slip is likely at the edges of the contact.

The pattern of micro-slip depends upon the relative elastic constants of the strip and rollers. If the materials are the same, or if the rollers are more flexible ($\beta \leqslant 0$) the tangential traction always acts inwards on the strip and a pattern of three slip regions similar to that with two dissimilar rollers in contact (Fig. 8.2) is obtained whatever the thickness of the strip. The distribution of traction and also the stress difference $|\sigma_x - \sigma_z|$ on the centre-plane of the strip are shown in Fig. 10.3 for $\beta = 0$, $b/a = 0.10$ and $\mu = 0.1$. Slip occurs in the same direction at entry and exit and a reversed slip region is located towards the exit. Slip affects neither the contact width a nor the indentation depth d, but the creep ratio is quite sensitive to the coefficient of friction (see Fig. 10.2).

When the strip is more flexible than the rollers ($\beta > 0$) the frictional traction acts outwards on thick strips and inwards on thin ones, so that the pattern of slip depends upon the strip thickness, but is similar to that shown in Fig. 10.3 if the strip is thin.

In the above discussion we have taken for granted that the strips and rollers have elastic constants which have a comparable magnitude, for example metal strips nipped by metal rollers. A somewhat different picture emerges when the rollers are relatively rigid compared with the strip, particularly if the strip is incompressible, for example rubber sheet nipped between metal rollers. With a sufficiently thick strip the contact stresses approach those for a rigid cylinder indenting an elastic half-space. A thin strip nipped between *frictionless* rollers is similar to an elastic layer supported on a frictionless base indented by a frictionless cylinder, which has been discussed in §5.8. But when friction between the roller and the strip is taken into account simple solutions based on homogeneous deformation are unsatisfactory.

Fig. 10.2. An elastic strip between elastic rollers: semi-contact-width a, penetration d and creep ratio ξ. ($C = 1, \beta = 0, \nu_1 = \nu_2 = 0.3$).

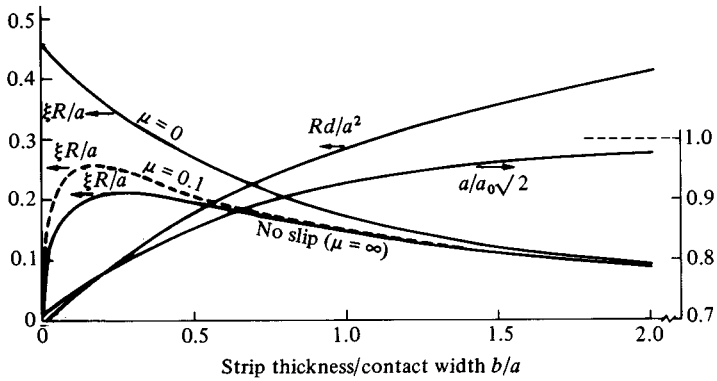

https://doi.org/10.1017/CBO9781139171731.011 Published online by Cambridge University Press

A complete numerical solution is presented in Fig. 10.4 for $C = 1000$ and $\nu_1 = 0.5$ assuming no slip. For an incompressible material in contact with a relatively rigid one $\beta = 0$, so that the half-space solution, which is the limit for $b \gg a$, does not involve any frictional traction and the stresses and deformation are given by Hertz. Thinner strips tend to be squeezed out longitudinally and inward acting tangential tractions arise. The ratio of $q(x)/p(x)$, shown in Fig. 10.4(b), indicates the magnitude of the coefficient of friction which is necessary to prevent slip at the edges of the contact. For $b \approx 0.25a$ the pressure distribution shown in Fig. 10.4(a) is approximately parabolic, as suggested by equation (5.71). For $b \approx 0.1a$ the pressure distribution for an incompressible material becomes bell-shaped, roughly as given by equation (5.75). Further

Fig. 10.3. An elastic strip between rollers ($C = 1, \beta = 0, \nu_1 = \nu_2 = 0.3$). ($a$) Distributions of pressure $p(x)$ and tangential traction $q(x)$. (b) Stress difference $|\sigma_x - \sigma_z|$.

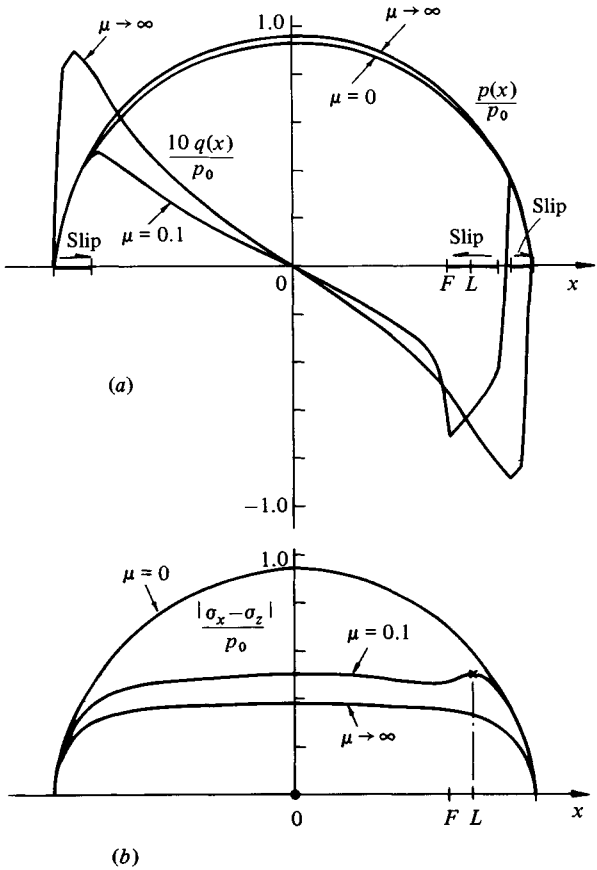

https://doi.org/10.1017/CBO9781139171731.011 Published online by Cambridge University Press

Fig. 10.4. An incompressible elastic strip nipped between relatively rigid rollers with no slip ($C = 1000, \beta = 0, \nu_1 = 0.5, \nu_2 = 0.3$). (*a*) Distributions of pressure and traction. (*b*) Ratio: $q(x)/p(x)$.

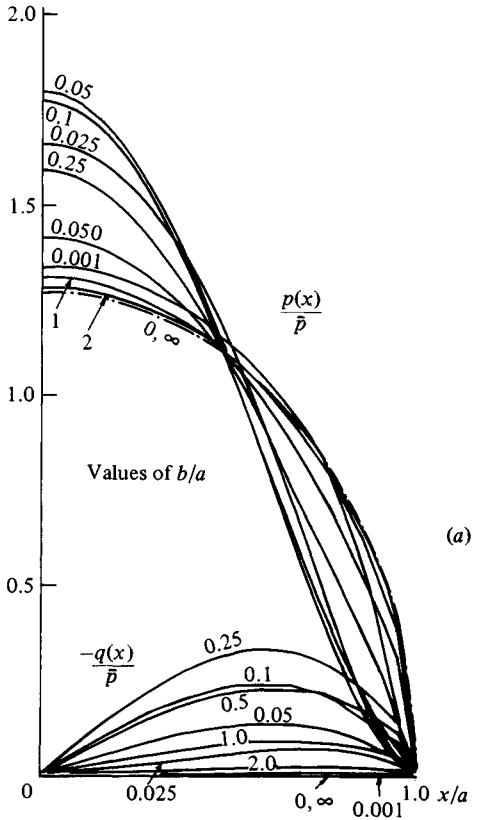

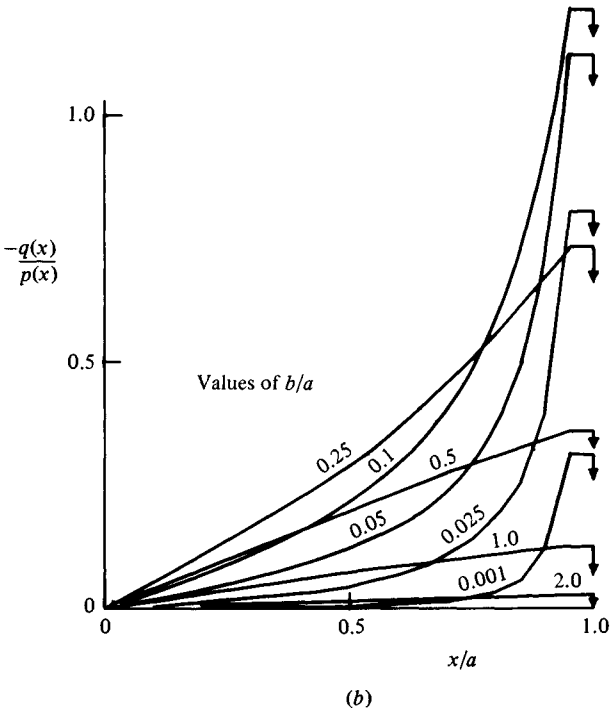

Fig. 10.5. An incompressible elastic strip between relatively rigid rollers ($C = 1000, \beta = 0, \nu_1 = 0.5, \nu_2 = 0.3$). Semi-contact-width a, penetration d and creep ratio ξ. Solid line – no slip ($\mu = \infty$); broken line – frictionless ($\mu = 0$).

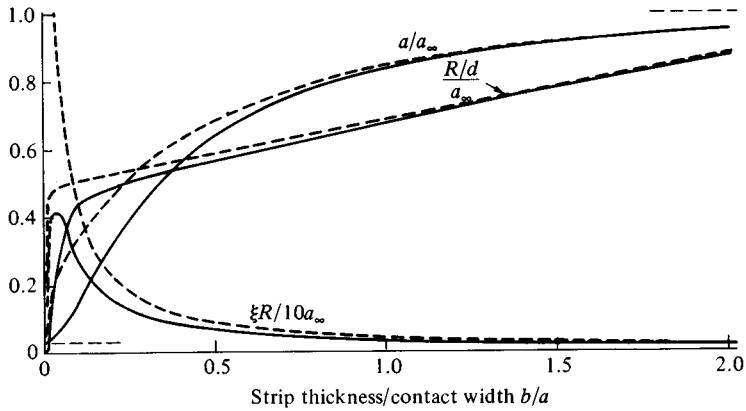

reduction in thickness of the strip results in deformation of the rollers becoming significant. In the limit when b is vanishingly small, the deformation is confined to the rollers, the stresses are again given by Hertz for the contact of two equal cylinders, so that the frictional traction also vanishes in this limit. The variations of contact width, penetration and creep ratio with strip thicknesses are plotted in Fig. 10.5.

10.2 Onset of plastic flow in a thin strip

In the metal industries thin sheet is produced from thick billets by plastic deformation in a rolling mill. We shall consider this process further in §3 but first we must investigate the conditions necessary to initiate plastic flow in a strip nipped between rollers. A thick billet is similar to a half-space so that the initial yield occurs (by the Tresca criterion) when the maximum elastic contact pressure p_0 reaches $1.67Y$ (eq. (6.4)), where Y is the yield stress of the billet in compression. A thin strip between rollers, as shown in Fig. 10.1, will yield when

$$|\sigma_x - \sigma_z|_{\max} = Y\dagger \tag{10.10}$$

With frictionless rollers σ_x is approximately zero and $\sigma_z = -p$, so that yield in this case occurs when $p_0 \approx Y$, which is lower than for a thick billet. However it

† This criterion assumes that σ_y is the intermediate principal stress. With very thin strips that is no longer the case so that yield, in fact, initiates by lateral spread. However plane strain conditions restrict such plastic deformation to a negligible amount.

https://doi.org/10.1017/CBO9781139171731.011 Published online by Cambridge University Press

is a fact of experience that very high contact pressures are necessary to cause plastic flow in a thin strip. The frictional traction acts inwards towards the mid-point of the contact (see eq. (10.9) for a strip which sticks to the rollers) and results in a compressive longitudinal stress σ_x which inhibits yield.

Detailed calculations of the stresses on the mid-plane of the strip have been made by Johnson & Bentall (1969) for $\mu = 0$, 0.1 and for no slip ($\mu \to \infty$). A typical variation of $|\sigma_x - \sigma_z|$ through the nip is shown in Fig. 10.3(*b*). The effect of friction on $|\sigma_x - \sigma_z|_{\max}$ is very marked. By using the yield criterion (10.10) the load to cause first yield P_Y is found for varying thicknesses of strip h and the results plotted non-dimensionally in Fig. 10.6. The influence of friction in producing a rise in the load to cause yield in thin strips is most striking.

The initiation of yield does not necessarily lead to measurable plastic deformation. If the plastic zone is fully contained by elastic material the plastic strains are restricted to an elastic order of magnitude. The point of initial yield (point of $|\sigma_x - \sigma_z|_{\max}$) in the strip lies towards the rear of the nip in the middle slip zone marked L in Fig. 10.3. In this slip zone the strip is moving faster than the rollers. If there is to be any appreciable permanent reduction in thickness of the strip it must also emerge from the nip moving faster than the rollers. For this to happen the second stick zone and the final reversed slip zone of the elastic solution (Fig. 10.3(*a*)) must be swept away. The middle slip zone,

Fig. 10.6. Load to cause first yield P_Y and the load to cause uncontained plastic reduction P_F in the rolling of strip of thickness h.

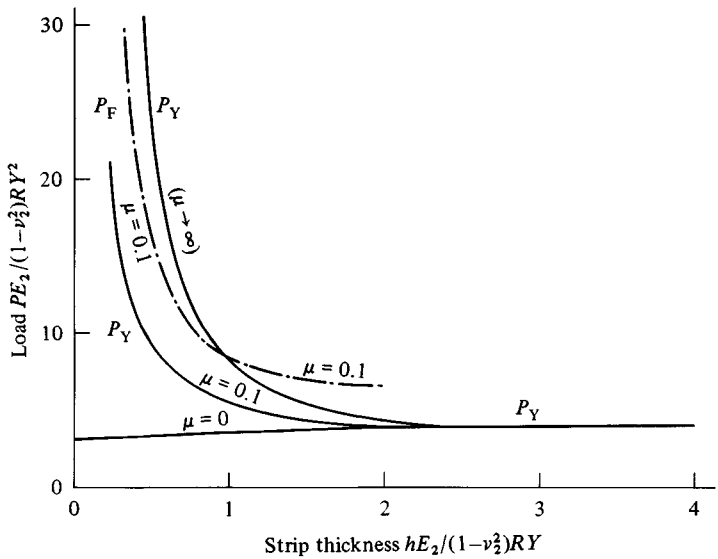

https://doi.org/10.1017/CBO9781139171731.011 Published online by Cambridge University Press

in which plastic reduction is taking place, will then extend to the exit of the nip. The distribution of traction and the corresponding variation in $|\sigma_x - \sigma_z|$ compatible with a single slip zone at exit have been calculated. $|\sigma_x - \sigma_z|_{\max}$ has equal maximum values at the beginning and end of the no-slip zone, so that plastic flow begins at F in Fig. 10.3. Putting $|\sigma_x - \sigma_y|_{\max} = Y$ in this case leads to a value of the load P_F at which uncontained plastic flow commences. The variation of P_F with strip thickness (taking $\mu = 0.1$) is included in Fig. 10.6. It shows that the load to initiate measurable plastic reduction is almost double that to cause first yield. The effect of friction in preventing the plastic flow of very thin strips is again clearly demonstrated. The superimposition of an external tension in the strip reduces the longitudinal compression introduced by friction and makes yielding easier.

10.3 Plastic rolling of strip

When a metal strip is passed through a rolling mill to produce an appreciable reduction in thickness, the plastic deformation is generally large compared with the elastic deformation so that the material can be regarded as being rigid-plastic. In the first instance the elastic deformation of the rolls may also be neglected. For continuity of flow, the rolled strip emerges from the nip at a velocity greater than it enters, which is in inverse proportion to its thickness if no lateral spread occurs. Clearly the question of sticking and slipping between the rolls and the strip, which has been prominent in previous chapters, arises in the metal rolling process. In hot rolling the absence of lubricant and the lower flow stress of the metal generally mean that the limiting frictional traction at the interface exceeds the yield stress of the strip in shear so that there is no slip in the conventional sense at the surface.

It is for the condition of no slip encountered in hot rolling that the most complete analyses of the process have so far been made. We saw in the previous section that interfacial friction inhibits plastic reduction, so that in cold rolling the strip is deliberately lubricated during its passage through the rolls in order to facilitate slip. At entry the strip is moving slower than the roll surfaces so that it slips backwards; at exit the strip is moving faster so that it slips fowards. At some point in the nip, referred to as the 'neutral point' the strip is moving with the same velocity as the rolls. At this point the slip and the frictional traction change direction. In reality, however, we should not expect this change to occur at a point. In the last section, when a thin *elastic* strip between *elastic* rollers was being examined, we saw that plastic deformation and slip would initiate at entry and exit; in between there is a region of no slip and no plastic deformation. It seems likely therefore that a small zone of no slip will continue to exist even when appreciable plastic reduction is taking place in the nip as a whole. Current

theories of cold rolling, which are restricted to the idea of a 'neutral point', must be regarded as 'complete slip' solutions in the sense discussed in Chapters 8 and 9.

The complete solution of a problem involving the plane deformation of a rigid-perfectly-plastic material calls for the construction of a slip-line field. So far this has been achieved only for the condition of no slip, which applies to hot rolling. Before looking at these solutions we shall examine the elementary theories, with and without slip, which derive from von Kármán (1925).

The geometry of the roll bite, neglecting elastic deformation, is shown in Fig. 10.7. The mean longitudinal (compressive) stress in the strip is denoted by $\bar{\sigma}_x$ and the transverse stress at the surface by $\bar{\sigma}_z$. Equilibrium of the element gives

$$\bar{\sigma}_z \, dx = (p \cos \phi + q \sin \phi) R \, d\phi \tag{10.11}$$

and

$$d(h\bar{\sigma}_x) = (p \sin \phi - q \cos \phi) 2R \, d\phi \tag{10.12}$$

In this simple treatment it is assumed that in the plastic zone $\bar{\sigma}_x$ and $\bar{\sigma}_z$ are

Fig. 10.7

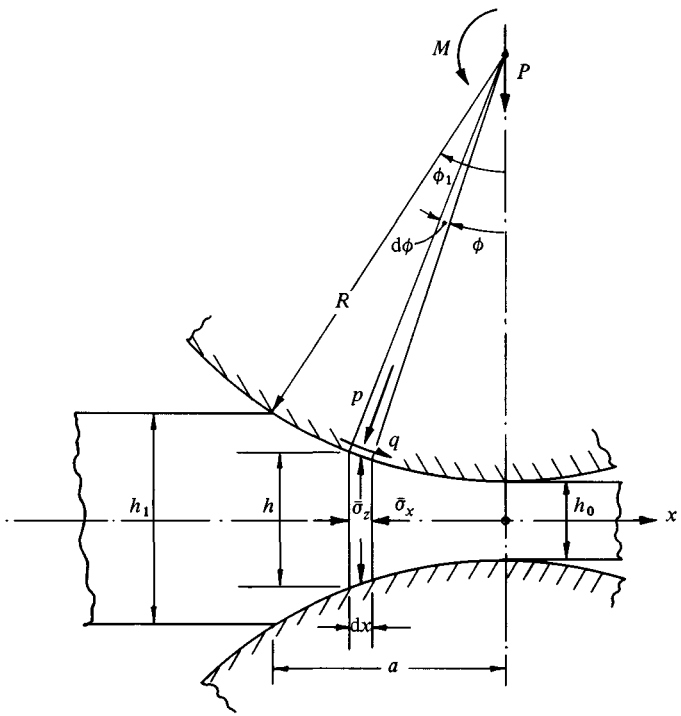

https://doi.org/10.1017/CBO9781139171731.011 Published online by Cambridge University Press

related by the yield criterion

$$\bar{\sigma}_z - \bar{\sigma}_x = 2k \tag{10.13}$$

This simplification implies a homogeneous state of stress in the element which is clearly not true at the surface of the strip where the frictional traction acts. Nevertheless by combining equations (10.11), (10.12) and (10.13) we obtain

$$\frac{\mathrm{d}}{\mathrm{d}\phi}\{h(p + q\tan\phi - 2k)\} = 2R(p\sin\phi - q\cos\phi) \tag{10.14}$$

which is von Kármán's equation. It is perfectly straightforward to integrate this equation numerically (see Alexander, 1972) to find the variation in contact pressure $p(\phi)$ once the frictional conditions at the interface are specified. Before electronic computers were available, however, various simplifications of von Kármán's equation were proposed to facilitate integration. For relatively large rolls it is reasonable to put $\sin\phi \approx \phi$, $\cos\phi \approx 1$ etc. and to retain only first order terms in ϕ. The roll profile is then approximated by

$$h \approx h_0 + R\phi^2 \approx h_0 + x^2/R \tag{10.15}$$

Making these approximations in (10.14), neglecting the term $q\tan\phi$ compared with p, and changing the position variable from ϕ to x give

$$h\frac{\mathrm{d}p}{\mathrm{d}x} = 4k\frac{x}{R} + 2q \tag{10.16}$$

In addition, it is consistent with neglecting second order terms in ϕ to replace h by the mean thickness $\bar{h}\,(=\frac{1}{2}(h_0 + h_i))$. To proceed, the frictional traction q must be specified.

(a) Hot rolling - no slip

For hot rolling, it is assumed that q reaches the yield stress k of the material in shear throughout the contact arc. Equation (10.16) then becomes

$$\bar{h}\frac{\mathrm{d}p}{\mathrm{d}x} = 2k\left(2\frac{x}{R} \pm 1\right) \tag{10.17}$$

The positive sign applies to the entry region where the strip is moving slower than the rolls and the negative sign applies to the exit. Integration of (10.17), taking $\bar{\sigma}_x = 0$ at entry and exit, gives the pressure distribution:

At entry

$$\frac{\bar{h}}{a}\left(\frac{p}{2k} - 1\right) = (1 + x/a) - \frac{a}{R}(1 - x^2/a^2) \tag{10.18a}$$

and at exit

$$\frac{\bar{h}}{a}\left(\frac{p}{2k} - 1\right) = -x/a + \frac{a}{R}\frac{x^2}{a^2} \tag{10.18b}$$

https://doi.org/10.1017/CBO9781139171731.011 Published online by Cambridge University Press

The pressure at the neutral point is common to both these equations, which locates that point at

$$\frac{x_n}{a} = -\tfrac{1}{2} + \frac{a}{2R} \tag{10.19}$$

The total load per unit width is then found to be

$$\frac{P}{ka} = \frac{1}{ka}\int_{-a}^{0} p(x)\,\mathrm{d}x \approx 2 + \frac{a}{\bar{h}}\left(\tfrac{1}{2} - \tfrac{1}{3}\frac{a}{R}\right) \tag{10.20}$$

and the moment applied to the rolls is found to be

$$\frac{M}{ka^2} = \frac{1}{ka^2}\int_{-a}^{0} xp(x)\,\mathrm{d}x \approx 1 + \tfrac{1}{4}\frac{a}{\bar{h}}\left(1 - \frac{a}{R}\right) \tag{10.21}$$

This analysis is similar to the theory of hot rolling due to Sims (1954), except for the factor $\pi/4$ which Sims introduces on the right-hand side of equation (10.13) to allow for the non-homogeneity of stress. It is clear from the above expressions for force and torque that the 'aspect ratio' $\bar{h}/a$ is the primary independent variable: the parameter a/R, which is itself small in the range of validity of this analysis (ϕ small), exerts only a minor influence. Equations (10.20) and (10.21) for force and torque are plotted as dotted lines in Fig. 10.10.

The approach outlined above, in which the yield condition (10.13) is applied to the *average* stresses acting on the section of strip, makes equation (10.14) for the contact forces statically determinate, but the actual distributions of stress and deformation within the strip remain unknown. In reality the stresses within the strip should follow a statically admissible slip-line field and the deformation should follow a hodograph which is compatible with that field. To ensure such compatibility is far from easy. It was first achieved by Alexander (1955) by using a graphical trial-and-error method for a single configuration ($\bar{h}/a = 0.19$, $a/R = 0.075$) and by assuming that

$$-k \leqslant q \leqslant +k$$

everywhere throughout the arc of contact. The slip-line field and hodograph are shown in Fig. 10.8(*b*) and (*c*). In the centre of the roll bite there is a cap of undeforming material attached to the roller over the arc *CD*. The tangential traction $|q| < k$ in this arc. There is also a thin sliver of undeforming material on the arc *AB* at entry. The material is deforming plastically in the zones *ABCNF* and *DEGN*. A velocity discontinuity follows the slip lines *AB*, *CN* and *ND*. There is 'quasi-slip' between the rolls and the strip on the areas *BC* and *DE* which takes the form of a 'boundary layer' of intense shear at the yield stress k. The state of stress in the strip is obtained by following the slip lines from the entry at *A* or the exit at *E*. At the neutral point *N* the stress is the

https://doi.org/10.1017/CBO9781139171731.011 Published online by Cambridge University Press

same from whichever end it is approached. The pressure distribution over the contact arc is shown by the full lines in Fig. 10.8 where it is compared with the simple theory given by equations (10.18) (shown dotted).

Slip-line fields for other geometric configurations have since been constructed by Crane & Alexander (1968) for thin strips and by Dewhurst *et al.* (1973) for thicker strips. It transpires that the form of the solution depends almost entirely upon the aspect ratio $\bar{h}/a$ and hardly at all upon the roll radius parameter a/R. A sample of the different fields is shown in Fig. 10.9. Alexander's original solution (Fig. 10.8) applies to thin strips. At a value of $\bar{h}/a \approx 0.29$ the quasi-

Fig. 10.8. Hot rolling of strip ($\bar{h}/a = 0.19$, $a/R = 0.075$). (*a*) Pressure distribution: solid line – from the slip-line field, Alexander (1955); broken line – from eq. (10.18); (*b*) Slip-line field (Mode I: $\bar{h}/a < 0.29$); (*c*) Hodograph.

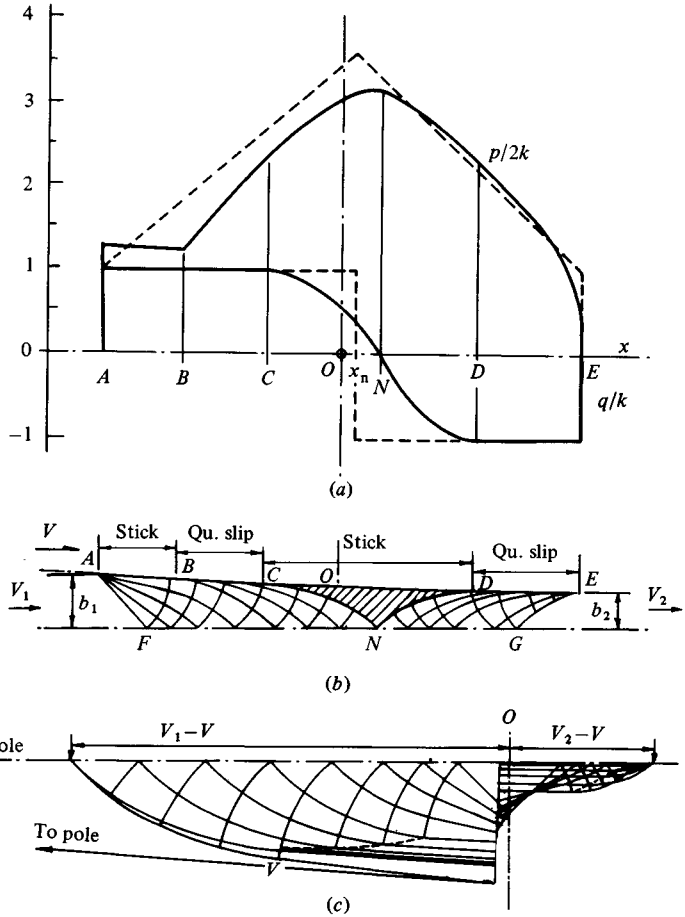

https://doi.org/10.1017/CBO9781139171731.011 Published online by Cambridge University Press

slip region BC just vanishes and the velocity discontinuity which follows the slip line AN now lies entirely within the material (Fig. 10.9(a)). A second critical aspect ratio occurs at $\bar{h}/a \approx 0.43$, when the quasi-slip region DE just vanishes and the rigid cap covers the whole arc of contact. The fields for greater values of $\bar{h}/a$ have been found by Dewhurst *et al.* (1973). The rigid cap AGE no longer penetrates to the centre-line of the strip, but a velocity discontinuity follows the slip lines AN and NE (Fig. 10.9(b)). At $\bar{h}/a \approx 0.72$, the arc GE contracts to a single point, whereupon the rigid zone takes the form shown in Fig. 10.9(c), with a velocity discontinuity along its boundary AE.

In view of the insensitivity of the fields to roll radius (i.e. to a/R), the roll force coefficient P/ka and torque coefficient M/ka^2 can be plotted as unique curves against the aspect ratio $\bar{h}/a$, as shown in Fig. 10.10. A minimum in both force and torque is obtained when the aspect ratio is about unity. With thin strips friction at the roll surfaces inhibits yield through high hydrostatic pressure in the centre of the roll bite; with thick strips, higher contact pressures are required to cause plastic flow through the thickness of the strip. When a further critical strip thickness is reached the roll pressure required to cause yield through the strip is greater than that to cause plastic flow only in the surface layers in the manner discussed in §9.3. By extending the slip-line field shown in Fig. 9.9(a) into the solid this critical thickness is found to be $\sim 8.8a$.

Fig. 10.9. Slip-line fields for hot rolling. (a) Mode II: $0.29 < \bar{h}/a < 0.43$; (b) Mode III: $0.43 < \bar{h}/a < 0.72$; (c) Mode IV: $0.72 < \bar{h}/a < 8.8$.

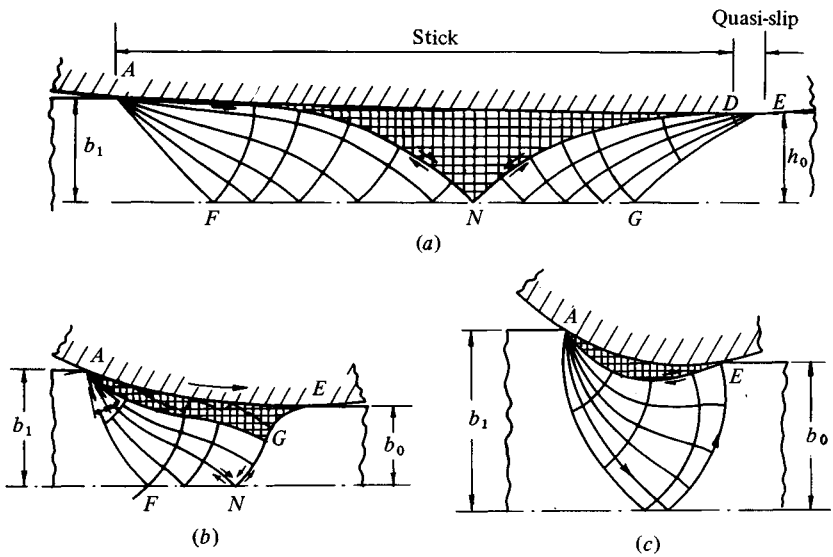

https://doi.org/10.1017/CBO9781139171731.011 Published online by Cambridge University Press

We must now examine the assumption that friction at the roll face is sufficient to prevent slip. In all cases the contact pressure is least at exit. In Crane & Alexander's solutions for thinner strips a coefficient of friction up to 0.7 is required to develop a traction of magnitude k in the zone DE (Fig. 10.8(b)).† In Dewhurst's solutions for thicker strips there is a small range of conditions, where G approaches E (Fig. 10.9(b)), which results in the roll pressure at E becoming negative. In practice some slip in the vicinity of E will remove this anomaly.

(b) Cold rolling - with slip

We turn now to the case of cold rolling, where the strip is taken to slip relative to the rolls at all points in the arc of contact, so that in equation (10.16) we write $q = \pm\mu p$. Replacing h by the mean thickness $\bar{h}$ gives a linear differential equation for the contact pressure:

$$\frac{\mathrm{d}(p/2k)}{\mathrm{d}X} \pm \frac{2\mu a}{\bar{h}}\left(\frac{p}{2k}\right) = \frac{2a^2X}{R\bar{h}} \tag{10.22}$$

where $X = x/a$. The negative sign applies at entry and the positive sign at exit.

† Denton & Crane (1972) have proposed a modified theory to allow for slip at exit.

Fig. 10.10. Variation of roll force P and roll torque M with aspect ratio $\bar{h}/a$. Solid line - from slip-line fields; broken line - eqs. (10.20) and (10.21); cross in circle - Alexander's solution (Fig. 10.8).

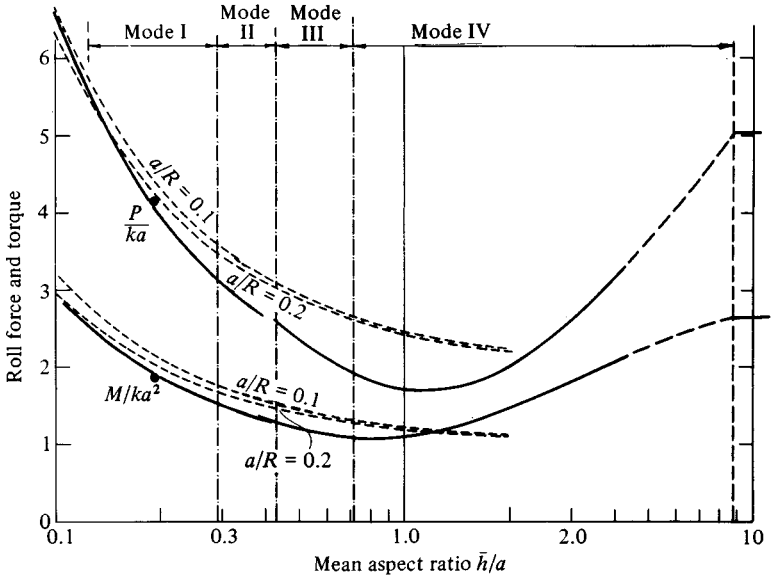

https://doi.org/10.1017/CBO9781139171731.011 Published online by Cambridge University Press

Integrating this equation, with $p/2k = 1$ at $X = 0$ and $X = -1$, gives the pressure in the entry zone to be

$$p/2k = \{1 + (\gamma/\lambda) - \gamma\}\, e^{\lambda(1+X)} - \gamma X - \gamma/\lambda \qquad (10.23a)$$

and in the exit zone

$$p/2k = (1 + \gamma/\lambda)\, e^{-\lambda X} + \gamma X - \gamma/\lambda \qquad (10.23b)$$

where $\lambda = (2\mu a/\bar{h})$ and $\gamma = (a/\mu R)$.

Equating the pressures given by (10.23*a* and *b*) yields the position of the neutral point:

$$x_n/a \equiv X_n \approx -\tfrac{1}{2} + \frac{\gamma}{2\lambda}(1 - e^{-\lambda/2}) \qquad (10.24)$$

Integrating the pressure over the arc of the contact gives an expression for the roll force:

$$\frac{P}{ka} = \frac{4(\lambda + \gamma)}{\lambda^2}\{\exp(-\lambda X_n) - 1\} + \gamma + (4\gamma X_n/\lambda) - 2\gamma X_n^2 \qquad (10.25)$$

Similarly for the roll moment:

$$\frac{M}{ka^2} = -\frac{4(\lambda + \gamma)}{\lambda^2} X_n \exp(-\lambda X_n) + \frac{\gamma}{\lambda}(1 - 4X_n^2 + 4X_n/\lambda)$$

$$+ \tfrac{2}{3}\gamma(1 + 2X_n^3) - 2/\lambda \qquad (10.26)$$

Provided that γ is not too large the values of roll force and roll moment given by the closed form expressions (10.24), (10.25) and (10.26) are very close to the numerical integration of von Kármán's equation (10.14) by Bland & Ford (1948). Owing to the dominance of the exponential terms in (10.25) and (10.26) it follows that the force and moment are governed predominantly by the aspect ratio parameter $\lambda(= 2\mu a/\bar{h})$ while the influence of $\gamma(= a/\mu R)$ is relatively small. The reduction in thickness of the strip through the rolls is related to the parameters λ and γ by

$$r \equiv \frac{h_i - h_o}{h_i} = \frac{\lambda\gamma}{2 + \lambda\gamma/2}$$

This brief résumé of the mechanics of plastic deformation of a strip passing between rolls has omitted many aspects of the problem which are important in the technological process. In cold rolling, strain hardening of the strip during deformation is usually significant. It can be included in the theory in an approximate way by permitting the yield stress k to be a prescribed function of deformation and hence of x in equation (10.17). Internal heating due to plastic work also influences the value of k. The rolls flatten appreciably by elastic

https://doi.org/10.1017/CBO9781139171731.011 Published online by Cambridge University Press

deformation. It is usual to calculate this by assuming that the contact pressure is distributed according to the Hertz theory, whereupon the rolls deform to a circular arc of modified radius R' which is related to R by equation (10.4). However the insensitivity of the deformation of the strip to roll radius suggests that this is not a serious effect except in the case of very thin hard strips where the elastic deformation of both strip and rolls is important. Finally thick billets will 'spread' laterally during rolling so that the deformation will not be plane, particularly towards the edges of the strip.

10.4 Lubrication of rollers

For engineering surfaces to operate satisfactorily in sliding contact it is generally necessary to use a lubricant. Even surfaces in nominal rolling contact, such as in ball bearings, normally experience some micro-slip, which necessitates lubrication if surface damage and wear are to be avoided. A lubricating fluid acts in two ways. Firstly it provides a thin protective coating to the solid surfaces, preventing the adhesion which would otherwise take place and reducing friction through an interfacial layer of low shear strength. This is the action known as 'boundary lubrication'; the film is generally very thin (it may be only a few molecules thick) and the behaviour is very dependent upon the physical and chemical properties of both the lubricant and the solid surfaces. The lubricant may act in a quite different way. A relatively thick coherent film is drawn in between the surfaces and sufficient pressure is developed in the film to support the normal load without solid contact. This action is known as 'hydrodynamic lubrication'; it depends only upon the geometry of the contact and the viscous flow properties of the fluid. The way in which a load-bearing film is generated between two cylinders in rolling and sliding contact will be described in this section. The theory can be applied to the lubrication of gear teeth, for example, which experience a relative motion which, as shown in §1.5, is instantaneously equivalent to combined rolling and sliding contact of two cylinders.

A thin film of incompressible lubricating fluid, viscosity η, between two solid surfaces moving with velocities V_1 and V_2 is shown in Fig. 10.11. With thin, nearly parallel films velocity components perpendicular to the film are negligible so that the pressure is uniform across the thickness. At low Reynolds' Number (thin film and viscous fluid) inertia forces are negligible. Then, for two-dimensional steady flow, equilibrium of the shaded fluid element gives

$$\frac{\partial p}{\partial x} = \frac{\partial \tau}{\partial z} = \frac{\partial}{\partial z}\left(\eta \frac{\partial v}{\partial z}\right) = \eta \frac{\partial^2 v}{\partial z^2} \tag{10.27}$$

where v is the stream velocity. Since $\partial p/\partial x$ is independent of z, equation (10.27) can be integrated with respect to z. Putting $v = V_2$ and V_1 at $z = 0$ and h gives

https://doi.org/10.1017/CBO9781139171731.011 Published online by Cambridge University Press

a parabolic velocity profile as shown, expressed by

$$v(z) = \frac{1}{2\eta}\frac{dp}{dx}(z^2 - hz) + (V_1 - V_2)(z/h) + V_2 \tag{10.28}$$

The volume flow rate F across any section of the film is

$$F = \int_0^h v(z)\,dz = -\frac{h^3}{12\eta}\left(\frac{dp}{dx}\right) + (V_1 + V_2)\frac{h}{2}$$

For continuity of flow F is the same for all cross-sections, i.e.

$$F = (V_1 + V_2)\frac{h^*}{2}$$

where h^* is the film thickness at which the pressure gradient dp/dx is zero. Eliminating F gives

$$\frac{dp}{dx} = 6\eta(V_1 + V_2)\left(\frac{h - h^*}{h^3}\right) \tag{10.29}$$

This is Reynolds' equation for steady two-dimensional flow in a thin lubricating film. Given the variation in thickness of the film $h(x)$, it can be integrated to give the pressure $p(x)$ developed by hydrodynamic action. For a more complete discussion of Reynolds' equation the reader is referred to books on lubrication (e.g. Cameron, 1966). We shall now apply equation (10.29) to find the pressure developed in a film between two rotating cylinders.

(a) Rigid cylinders

The narrow gap between two rotating rigid cylinders is shown in Fig. 10.12. An ample supply of lubricant is provided on the entry side. Within the

Fig. 10.11

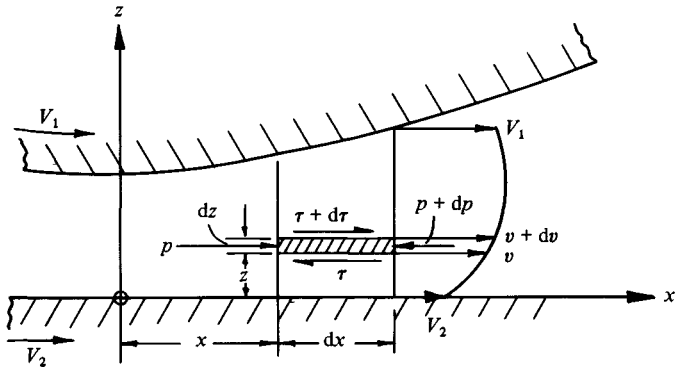

https://doi.org/10.1017/CBO9781139171731.011 Published online by Cambridge University Press

region of interest the thickness of the film can be expressed by

$$h \approx h_0 + x^2/2R \tag{10.30}$$

where $1/R = 1/R_1 + 1/R_2$ and h_0 is the thickness at $x = 0$. Substituting (10.30) into (10.29) gives

$$\frac{dp}{dx} = \frac{6\eta(V_1 + V_2)}{h_0^2} \left\{ \frac{1 - (h^*/h_0) + (x^2/2Rh_0)}{(1 + x^2/2Rh_0)^3} \right\} \tag{10.31}$$

By making the substitution $\gamma = \tan^{-1}\{x/(2Rh_0)^{1/2}\}$ equation (10.31) can be integrated to give an expression for the pressure distribution:

$$\frac{h_0^2}{(2Rh_0)^{1/2}} \frac{p}{6\eta(V_1 + V_2)} = \frac{\gamma}{2} + \frac{\sin 2\gamma}{4} - \sec^2 \gamma^* \left(\frac{3\gamma}{8} + \frac{\sin 2\gamma}{4} + \frac{\sin 4\gamma}{32} \right) + A \tag{10.32}$$

where $\gamma^* = \tan^{-1}\{x^*/(2Rh_0)^{1/2}\}$ and x^* is the value of x where $h = h^*$ and $dp/dx = 0$. The values of γ^* and A are found from end conditions.

We start by taking zero pressure at distant points at entry and exit, i.e. $p = 0$ at $x = \pm\infty$. The resulting pressure distribution is shown by curve A in

Fig. 10.12. Lubrication of rigid rollers. Broken line – pressure distribution with a complete film. Solid line – pressure distribution without negative pressure.

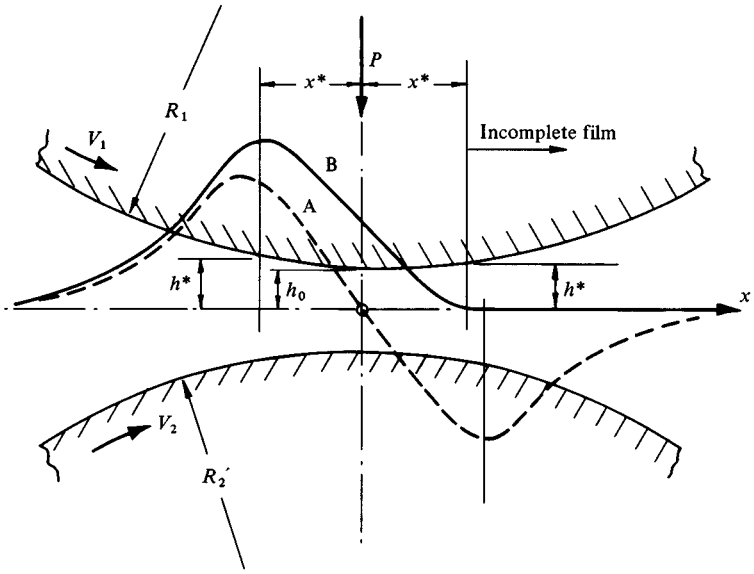

https://doi.org/10.1017/CBO9781139171731.011 Published online by Cambridge University Press

Fig. 10.12. It is positive in the converging zone at entry and equally negative in the diverging zone at exit. The total force P supported by the film is clearly zero in this case. However this solution is unrealistic since a region of large negative pressure cannot exist in normal ambient conditions. In practice the flow at exit breaks down into streamers separated by fingers of air penetrating from the rear. The pressure is approximately ambient (i.e. zero) in this region. The precise point of film breakdown is determined by consideration of the three-dimensional flow in the streamers and is influenced by surface tension forces. However it has been found that it can be located with reasonable success by imposing the condition

$$\frac{dp}{dx} = p = 0$$

at that point. When this condition, together with $p = 0$ at $x = -\infty$ is imposed on equation (10.32) it is found that $\gamma^* = 0.443$, whence $x^* = 0.475(2Rh_0)^{1/2}$. The pressure distribution is shown by curve B in Fig. 10.12. In this case the total load supported by the film is given by

$$P = \int_{-\infty}^{x^*} p(x)\,dx = 2.45(V_1 + V_2)R\eta/h_0 \tag{10.33}$$

In most practical situations it is the load which is specified; equation (10.33) then enables the minimum film thickness h_0 to be calculated. For effective hydrodynamic lubrication h_0 must not be less than the height of the inevitable surface irregularities. We see from equation (10.33) that the load-bearing capacity of the film is generated by *rolling* action characterised by the combined velocities $(V_1 + V_2)$. If the cylinders rotate at the same peripheral speed in *opposite* directions $(V_1 + V_2)$ is zero, no pressure is developed and the film collapses.

(b) Elastic cylinders

At all but the lightest loads the cylinders deform elastically in the pressure zone so that the expression for film profile becomes

$$h(x) = h_0 + x^2/2R + \{\bar{u}_{z1}(x) - \bar{u}_{z1}(0)\} + \{\bar{u}_{z2}(x) - \bar{u}_{z2}(0)\}$$

where the normal elastic displacements of the two surfaces $\bar{u}_{z1}$ and $\bar{u}_{z2}$ are given by equation (2.24*b*). Thus

$$h(x) = h_0 + (x^2/2R) - \frac{2}{\pi E^*}\int_{-\infty}^{\infty} p(s)\ln\left|\frac{x-s}{s}\right| ds \tag{10.34}$$

This equation and Reynolds' equation (10.29) provide a pair of simultaneous equations for the film shape $h(x)$ and the pressure $p(x)$. They can be combined

https://doi.org/10.1017/CBO9781139171731.011 Published online by Cambridge University Press

into a single integral equation for $h(x)$ which has been solved numerically by Herrebrugh (1968). The deformed shape is shown in Fig. 10.13(b). This film shape is then substituted into Reynolds' equation to find the pressure distribution $p(x)$, as shown in Fig. 10.13(a). The solution depends upon a single non-dimensional parameter $J \equiv \{P^2/\eta R(V_1 + V_2)\pi E^*\}^{1/2}$, which is a measure of the ratio of the pressure generated hydrodynamically in the film to the pressure to produce the elastic distortion. The parameter is zero for rigid cylinders and increases with increasing elasticity. It is evident from Fig. 10.13 that the effect of elastic deformation is to produce a film which is convergent over most of its effective length like a tilting pad thrust bearing. On the other hand, as the

Fig. 10.13. Lubrication of elastic rollers with an isoviscous lubricant. A: $J = 0$ (rigid), B: $J = 0.536$, C: $J = 7.42$, D: $J = 143$. (a) Pressure distribution $p(x)$; (b) film shape $h(x)$.

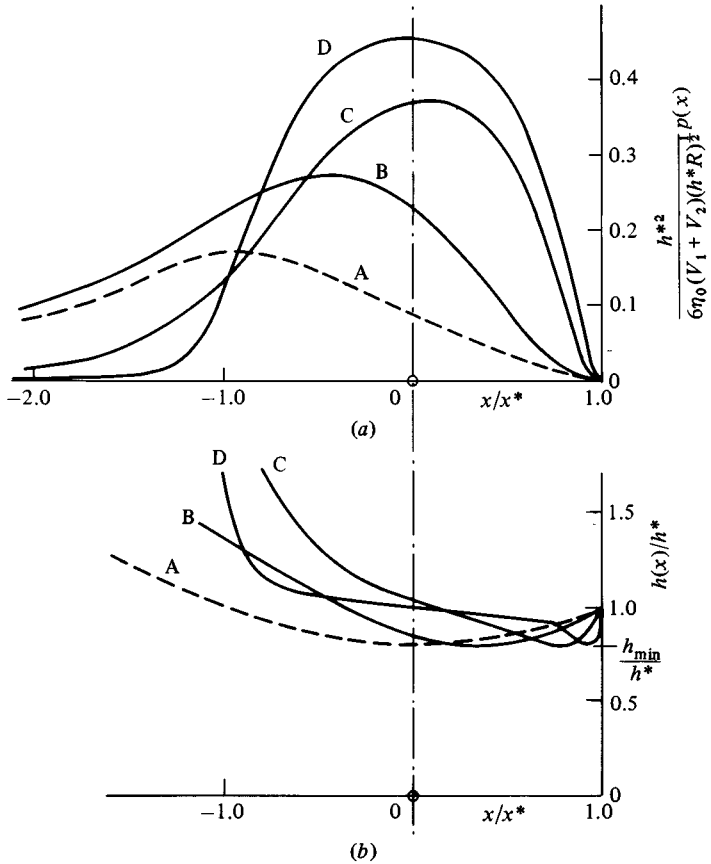

https://doi.org/10.1017/CBO9781139171731.011 Published online by Cambridge University Press

elastic flattening becomes large compared with the film thickness, the pressure distribution approaches that of Hertz for unlubricated contact.

From the point of view of effective lubrication it is the minimum film thickness $h_{\min}$ which is important. In all cases $h_{\min} \approx 0.8h^*$. The variation in the non-dimensional film thickness $H \equiv Ph_{\min}/\eta R(V_1 + V_2)$ with the parameter J is given in Table 10.1. For rigid cylinders ($J = 0$) the minimum thickness is h_0, given by equation (10.33). We see from the table that, by permitting a more favourable shape for generating hydrodynamic pressure, elastic rollers give thicker films under the same conditions of speed and loading.

This mode of lubrication behaviour in which the elastic deformation of the solid surface plays a significant role in the process is known as *elastohydrodynamic* lubrication. (See Dowson & Higginson, 1977).

(c) Variable viscosity

So far we have considered the viscosity η to be a constant property of the lubricating fluid, but in fact the viscosity of most practical lubricants is very sensitive to changes in pressure and temperature. In a non-conforming contact the pressures tend to be high so that it is not surprising that the increase in vicosity with pressure is also a significant factor in elastohydrodynamic lubrication. Particularly during sliding, frictional heating causes a rise in temperature in the film which reduces the viscosity of the film. However, for reasons which will become apparent later, it is possible to separate the effects of pressure and temperature. To begin with, therefore, we shall consider an isothermal film in which the variation in viscosity with pressure is given by the equation

$$\eta = \eta_0 \, e^{\alpha p} \tag{10.35}$$

where η_0 is the viscosity at ambient pressure and temperature and α is a constant pressure coefficient of viscosity. This is a reasonable description of the observed variation in viscosity of most lubricants over the relevant pressure range. Substituting this relationship into Reynolds' equation (10.29) gives

$$e^{-\alpha p} \frac{dp}{dx} = 6\eta_0(V_1 + V_2)\left(\frac{h - h^*}{h^3}\right) \tag{10.36}$$

Table 10.1

$J \equiv \left\{\dfrac{P^2}{\eta R(V_1 + V_2)\pi E^*}\right\}^{1/2}$	0 (rigid)	0.536	2.34	7.42	26.9	143
$H \equiv \dfrac{Ph_{\min}}{\eta R(V_1 + V_2)}$	2.45	2.91	4.11	6.05	9.51	17.6

https://doi.org/10.1017/CBO9781139171731.011 Published online by Cambridge University Press

This modified Reynolds' equation for the hydrodynamic pressure in the field must be solved simultaneously with equation (10.34) for the effect of elastic deformation on the film shape. Numerical solutions to this problem have been obtained by Dowson *et al.* (1962). Typical film shapes and pressure distributions are shown in Fig. 10.14. The inclusion of the pressure viscosity coefficient α introduces a second non-dimensional parameter

$$K \equiv \{\alpha^2 P^3/\eta_0 R^2 (V_1 + V_2)\}^{1/2}$$

Comparing Figs. 10.13 and 10.14 shows that the pressure-viscosity effect has a marked influence on the behaviour. Over an appreciable fraction of the contact area the film is approximately parallel. This follows from equation (10.36). When the exponent αp exceeds unity the left-hand side becomes small, hence $h - h^*$ becomes small, i.e. $h \approx h^* =$ constant. The corresponding pressure distribution is basically that of Hertz for dry contact, but a sharp pressure peak occurs on the exit side, followed by a rapid drop in pressure and thinning of the film where the viscosity falls back to its ambient value η_0. Dowson *et al.* (1962) have shown that allowing for the compressibility of the lubricant attenuates the peak to some extent. A more realistic equation for the variation of viscosity

Fig. 10.14. Numerical solution of the elastohydrodynamic eqs. (10.34) and (10.36) from Dowson *et al.* (1962). Values of J and K: A 0.54, 18; B 1.7, 58; C 5.4, 180; D 17, 580; E 54, 1800; F ∞, ∞ (dry). (*a*) Pressure distribution, (*b*) Film shape.

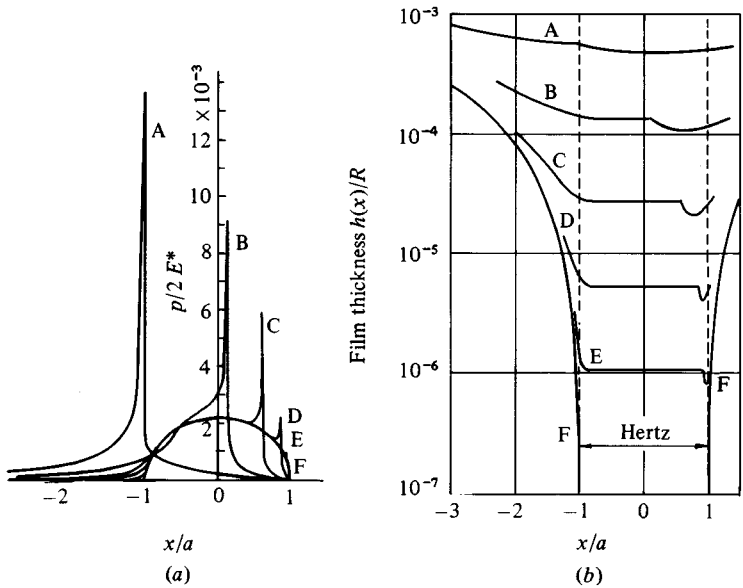

https://doi.org/10.1017/CBO9781139171731.011 Published online by Cambridge University Press

with pressure together with some shear thinning of the lubricant is likely to reduce the intensity of the theoretical peak still further.

Nevertheless these characteristic features of highly loaded elastohydrodynamic contacts - a roughly parallel film with a constriction at the exit and a pressure distribution which approximates to Hertz but has a sharp peak near the exit - are now well established by experiment (see Crook, 1961; and Hamilton & Moore, 1971). The minimum film thickness is about 75% of the thickness in the parallel section.

In the range of their computations Dowson & Higginson's results can be expressed approximately by

$$H = 1.4K^{0.54}J^{0.06} \tag{10.37}$$

Under these conditions the film thickness is weakly dependent upon the elasticity parameter J. The question now arises: under what conditions is it appropriate to neglect elastic deformation and/or variable viscosity? This question has been considered by Johnson (1970*b*) which has led to the following guidelines. If the parameter $J < 0.3$ and $K < 0.7$ deformation and variable viscosity are negligible and the analysis in section (*a*) is adequate. The relative importance of variable viscosity and elasticity depends upon a parameter $(K^2/J^3)^{1/4}$. For values of this parameter less than about 0.4, changes in viscosity are negligible compared with elastic effects and Herrebrugh's analysis given in section (*b*) above is appropriate. This condition is likely to be met only with rubber or other highly elastic polymers (using typical lubricants) where large elastic deformations are obtained at relatively low pressures. Dowson & Higginson's results on the other hand require that $(K^2/J^3)^{1/4}$ should have a value in excess of about 1.5. This is the engineering regime of metal surfaces lubricated with typical mineral oils. Values of non-dimensional film thickness H with appropriate values of K, taking $(K^2/J^3)^{1/4} = 4$, are given in Table 10.2.

Table 10.2

$\left(\frac{K^2}{J^3}\right)^{1/4} = 4$							
	K	0 (isoviscous)	50	100	500	1000	5000
	J	0 (rigid)	2.1	3.4	9.9	15.8	46.2
Dowson & Higginson eq. (10.37)	H	2.45	12	18	46	68	175
Grubin eq. (10.43)	H	–	14	21	53	80	203

https://doi.org/10.1017/CBO9781139171731.011 Published online by Cambridge University Press

It is evident from this table that the combined effect of elastic deformation and variable viscosity is to increase the minimum film thickness by one to two orders of magnitude compared with the equivalent thickness for an isoviscous fluid and rigid rollers.

Although solutions of the elastohydrodynamic equations on the computer provide valuable data, they do not give the same insight into the mechanics of the process as an early approximate treatment by Grubin (1949), extended later by Greenwood (1972). Grubin realised that in a high pressure contact with a pressure-sensitive lubricant, such that αp_0 appreciably exceeds unity ($\alpha p_0 > 5$, say), Reynolds' equation (10.36) demands that the film must be nearly parallel in the high pressure region with a thickness $h \approx h^*$. He assumed therefore that the elastic deformation of the rollers is the same as in dry contact and that a parallel film of thickness h^* exists over the length $2a$ of the Hertz flat. The elastic displacements outside the parallel zone are found by substituting the Hertz pressure distribution into equation (2.24*b*), whereupon the film shape in the entry zone is given by

$$h(x) = h^* + \frac{a}{2R}\left[\frac{x}{a}\left(\frac{x^2}{a^2} - 1\right)^{1/2} - \ln\left\{\frac{x}{a} + \left(\frac{x^2}{a^2} - 1\right)^{1/2}\right\}\right]$$

A good approximation to this cumbersome expression in the relevant region is

$$h(x) \approx h^* + \frac{a^2}{3R}\left(\frac{2\chi}{a}\right)^{3/2} \tag{10.38}$$

where $\chi\ (= -(x + a))$ is measured from the edge of the parallel zone $x = -a$ (see Fig. 10.15). We now define a reduced pressure p' by

$$p' = (1 - e^{-\alpha p})/\alpha$$

or

$$p = -\frac{1}{\alpha}\ln(1 - \alpha p') \tag{10.39}$$

Substituting (10.38) and (10.39) into the hydrodynamic equation (10.36) gives

$$\frac{dp'}{d\chi} = -6\eta_0(V_1 + V_2)\left[\frac{(a^2/3R)(2\chi/a)^{3/2}}{\{(a^2/3R)(2\chi/a)^{3/2} + h^*\}^3}\right]$$

or, by writing $(2\sqrt{2}\,a^2/3Rh^*)^{2/3}(\chi/a) = \xi$,

$$\frac{dp'}{d\xi} = -6\eta_0(V_1 + V_2)\left(\frac{3Rh^*}{2\sqrt{2}\,a^2}\right)^{2/3}\frac{a}{h^{*2}}\frac{\xi^{3/2}}{(\xi^{3/2} + 1)^3} \tag{10.40}$$

This equation can be integrated directly for the build-up in pressure in the entry region, taking $p' = 0$ at $\xi = \infty$. At the start of the parallel section ($\xi = 0$)

$$p'_0 = 6\eta_0(V_1 + V_2)\left(\frac{2Rh^*}{2\sqrt{2}\,a^2}\right)^{2/3}\frac{a}{h^{*2}}\int_0^\infty \frac{\xi^{3/2}}{(\xi^{3/2} + 1)^3}\,d\xi$$

https://doi.org/10.1017/CBO9781139171731.011 Published online by Cambridge University Press

Now

$$\int_0^\infty \frac{\xi^{3/2}\,d\xi}{(\xi^{3/2}+1)^3} = 0.255$$

so that

$$h^* = 1.417\left\{\frac{\eta_0(V_1+V_2)}{p_0'}\right\}^{3/4}\frac{R^{1/2}}{a^{1/4}} \tag{10.41}$$

It is clear from equation (10.39) that the reduced pressure p' cannot exceed $1/\alpha$ otherwise the actual pressure becomes infinite. This condition sets a lower limit on the value of the film thickness h^*, hence

$$h^* > 1.417\,\{\alpha\eta_0(V_1+V_2)\}^{3/4}R^{1/2}a^{-1/4} \tag{10.42}$$

Furthermore, since Grubin's treatment is restricted to high pressures in which αp_0 appreciably exceeds unity, $\alpha p_0'$ will approach unity very closely and hence the right-hand side of (10.42) will be a good approximation to the actual thickness of the film in the parallel section. Remembering that, by Hertz, $a^2 = 4PR/\pi E^*$, equation (10.42) can be rewritten in the form

$$H = 0.89K^{0.75}J^{-0.25} \tag{10.43}$$

Fig. 10.15. Elastohydrodynamic lubrication of rollers: the Grubin–Greenwood idealisation.

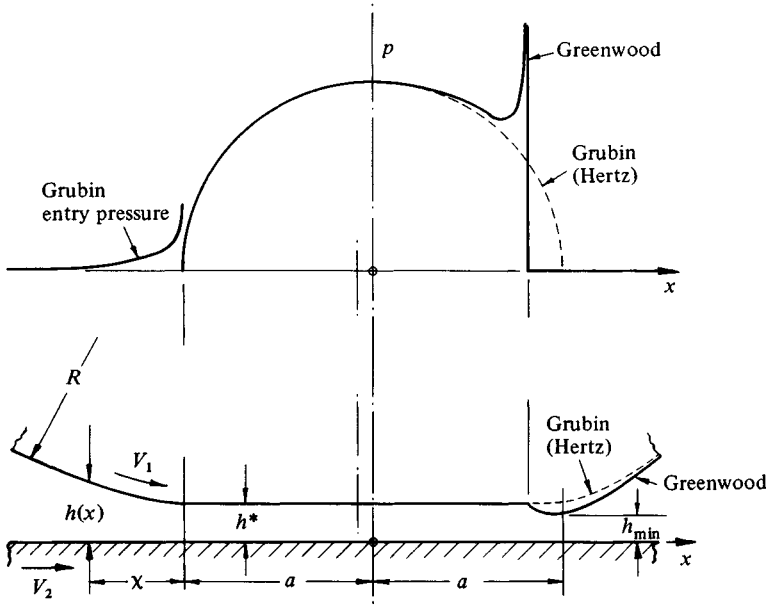

https://doi.org/10.1017/CBO9781139171731.011 Published online by Cambridge University Press

Values of H deduced from this approximate expression are compared with those from the computer solutions in Table 10.2. The agreement is reasonably good.

The analysis so far has been concerned entirely with the converging region at entry and has demonstrated that the film thickness in the parallel zone is determined to good approximation by the flow in this region. It also shows that the film thickness is relatively insensitive to load. Increasing the load increases the length $2a$ of the parallel zone, but this has only a marginal effect on the shape of the entry zone and hence upon the film thickness.

The assumption in Grubin's theory of a parallel zone of thickness approximately equal to h^* cannot be correct at exit. Here the pressure gradient must become negative, for which Reynolds' equation demands that h must fall below h^*. This is the reason for the constriction in the film at exit which is a feature of all elastohydrodynamic film profiles. Greenwood (1972) has extended Grubin's analysis to cover the exit zone by postulating a slightly shortened parallel zone. The pressure distribution within the parallel region required to produce this form of elastic deformation is found from equation (2.45). It is illustrated in Fig. 10.15. The elastic pressure is zero at the entry to the parallel zone, but rises to a sharp singularity at the end of the flat followed by a constriction in the film. Both the pressure spike and the constriction in the film reflect the characteristic features of the computer solutions for values of $\alpha p_0 > 5$. At practical speeds the entry conditions are independent of the exit conditions so that the value of h^* given by equation (10.42) is unchanged by Greenwood's modification. The minimum thickness which occurs in the exit constriction is found to be 75–80% of h^*.

The mechanism of elastohydrodynamic lubrication with a pressure-dependent lubricant is now clear. Pressure develops by hydrodynamic action in the entry region accompanied by a very large increase in viscosity. The film thickness at the end of the converging zone is limited by the necessity of maintaining a finite pressure. This condition virtually determines the film thickness in terms of the speed, roller radii and the viscous properties of the lubricant. Increasing the load increases the elastic flattening of the rollers with only a minor influence on the film thickness. The highly viscous fluid passes through the parallel zone until the pressure and viscosity collapse at the exit, which requires a thinning of the film. The inlet and exit regions are effectively independent; they meet at the end of the parallel zone with a discontinuity in slope of the surface which is associated with a sharp peak in pressure.

We can now return to the effect of temperature on viscosity. Viscous dissipation occurs in the entry region even without sliding, i.e. when $V_1 = V_2$. The dissipation gives rise to a resistance to rolling (Crook, 1963) and to a rise in temperature, which both increase with viscosity and rolling speed. Studies of

viscous heating at entry by Murch & Wilson (1975) have shown that it will not affect the film thickness appreciably until the parameter $(V_1 + V_2)^2(\mathrm{d}\eta_0/\mathrm{d}\theta)/K$ exceeds unity, where $(\mathrm{d}\eta_0/\mathrm{d}\theta)$ is the rate of change of viscosity with temperature and K is the thermal conductivity of the lubricant. Experiments have demonstrated that the appropriate values of η_0 and α to use in the theory are those at the temperature of the rolling surfaces.

When sliding accompanies rolling ($V_1 \neq V_2$) the whole film is sheared, giving rise to a resultant tractive force and much more severe viscous heating than in pure rolling. The value of the traction and the consequent temperature rise depend upon the shear properties of the lubricant in the high-pressure zone. There is clear evidence of non-Newtonian behaviour in this region and appropriate constitutive equations for the fluid at high pressure, such as those suggested by Johnson & Tevaarwerk (1977), are necessary in order to predict the tractive forces. Such calculations are beyond the scope of this book. Fortunately the film is established in the entry zone and shear heating in the parallel zone occurs too late to affect its thickness appreciably. Measurements of the film thickness (*a*) by Dyson *et al.* (1956) using electrical capacitance and (*b*) by Wymer & Cameron (1974) using optical interferometry give good support for the isothermal theory both with and without sliding.

The elastohydrodynamic lubrication of point contacts has been studied by Archard & Cowking (1956), Cheng (1970) and Hamrock & Dowson (1977) leading to formulae for the film thickness.